

Seismic analysis of 70 Ophiuchi A: A new quantity proposed

Y. K. Tang ^{a,c}, S. L. Bi ^{b,a} and N. Gai ^{a,c}

^a*National Astronomical Observatories/Yunnan Observatory, Chinese Academy of Sciences, Kunming 650011, P. R. China*
e-mail: bisl@bnu.edu.cn; tangyanke@ynao.ac.cn

^b*Department of Astronomy Beijing Normal University, Beijing 100875, P. R. China*

^c*Graduate School of the Chinese Academy of Sciences, Beijing 100039, P. R. China*

Abstract

The basic intent of this paper is to model 70 Ophiuchi A using the latest asteroseismic observations as complementary constraints and to determine the fundamental parameters of the star. Additionally, we propose a new quantity to lift the degeneracy between the initial chemical composition and stellar age. Using the Yale stellar evolution code (YREC7), we construct a series of stellar evolutionary tracks for the mass range $M = 0.85 - 0.93 M_{\odot}$ with different composition Y_i ($0.26 - 0.30$) and Z_i ($0.017 - 0.023$). Along these tracks, we select a grid of stellar model candidates that fall within the error box in the HR diagram to calculate the theoretical frequencies, the large- and small- frequency separations using the Guenther's stellar pulsation code. Following the asymptotic formula of stellar p -modes, we define a quantity r_{01} which is correlated with stellar age. Also, we test it by theoretical adiabatic frequencies of many models. Many detailed models of 70 Ophiuchi A have been listed in Table 3. By combining all non-asteroseismic observations available for 70 Ophiuchi A with these seismological data, we think that Model 60, Model 125 and Model 126, listed in Table 3, are the optimum models presently. Meanwhile, we predict that the radius of this star is about $0.860 - 0.865 R_{\odot}$ and the age is about $6.8 - 7.0$ Gyr with mass $0.89 - 0.90 M_{\odot}$. Additionally, we prove that the new quantity r_{01} can be a useful indicator of stellar age.

Key words: Stars: oscillations; Stars: evolution; Stars: individual: 70 Ophiuchi A

1 Introduction

The solar five-minute oscillations have led to a wealth of information about the internal structure of the Sun. These results stimulated various attempts to detect solar-like oscillations for a handful of solar-type stars. Individual p -mode frequencies have been identified for a few stars: α Cen A (Bouchy and Carrier, 2002; Bedding

et al., 2004), α Cen B (Carrier and Bourban, 2003a; Kjeldsen et al., 2005), μ Arae (Bouchy et al., 2005), HD 49933 (Mosser et al., 2005), β Vir (Martić et al., 2004a; Carrier et al., 2005b), Procyon A (Martić et al., 2004b; Eggenberger et al., 2004a), η Bootis (Kjeldsen et al., 2003; Carrier et al., 2005a), β Hyi (Bedding et al., 2001; Carrier et al., 2001) and δ Eri (Carrier et al., 2003b). Based on these asteroseismic data, numerous theoretical analyses have been performed in order to determine precise global stellar parameters and to test the various complicating physical effects on the stellar structure and evolutionary theory (Thévenin et al., 2002; Eggenberger et al., 2004b, 2005; Kervella et al., 2004; Miglio and Montalbán, 2005; Provost et al., 2004, 2006).

Recently, Carrier and Eggenberger (2006) detected solar-like oscillations on the K0 V star 70 Ophiuchi A (HD 165341), and identified some possible existing frequencies. They obtained the large separation $\Delta\nu = 161.7 \pm 0.3 \mu\text{Hz}$ by observation over 6 nights with HARPS. The spectroscopic visual binary system 70 Ophiuchi is one of our nearest neighbors (5 pc) and is among the first discovered binary stars. It was observed first by Herschel in 1779. So 70 Ophiuchi A is famous as the primary of a visual and spectroscopic binary system in the solar neighborhood. Although many observation data have been obtained since 1779, the theoretical analysis of 70 Ophiuchi A has only been made by Fernandes et al. (1998). By a calibration method which take into account the simultaneous evolution of the two members of the binary system, they analyzed the 70 Ophiuchi A by means of standard evolutionary stellar models using the CESAM code bf (Morel, 1997) without microscopic diffusion. They found that the metallicity of 70 Ophiuchi A is very close to the solar one, the values of mixing-length parameter α and helium abundance Y are near the Sun. They thought that the star is younger than the Sun and 3 ± 2 Gyr is probably an limit considering the age versus stellar rotation relation with its rotation velocity ($v\sin i \approx 16 \text{ km s}^{-1}$).

The aim of our paper is to present the model which can be constrained by these seismology data. The observational constraints available for 70 Ophiuchi A are summarized in Sect. 2, while the numerical calculations are presented in Sect. 3. The seismic analyses are carried out and a new quantity r_{01} as a indication of stellar age is proposed in Sect. 4. Finally, the discussion and conclusions are given in Sect. 5.

2 Observational Constraints

2.1 Non-asteroseismic observation constraints

The mass of this star was investigated by Batten et al. (1984), Heintz et al. (1988), Fernandes et al. (1998) and Pourbaix et al. (2000), respectively. In the paper, we

Table 1
Non-asteroseismic observational data of 70 Ophiuchi A.

Observable	Value	Source
Mass M/M_{\odot}	0.89 ± 0.04	(1)
Effective temperature $T_{eff}(\text{K})$	5322 ± 20	(2)
Luminosity $\log(L/L_{\odot})$	-0.29 ± 0.03	(1)
Metallicity $[Fe/H]_s$	0.0 ± 0.1	(1)
Surface heavy element abundance $[Z/X]_s$	0.02365 ± 0.00535	(3)

References.—(1) Fernandes et al. (1998), (2) Gray and Johnson (1991), (3) this paper.

adopt the value of mass deduced from Fernandes et al. (1998). The effective temperature was determined by Gray and Johnson (1991). So far, the metallicity obtained by observation are $[Fe/H] = -0.05$ (Peterson, 1978) and $[Fe/H] = 0.00$ (Perrin et al., 1975). We choose the $[Fe/H] = 0.0 \pm 0.1$ as a representative value according to Fernandes et al. (1998).

The mass fraction of heavy elements, Z , was derived assuming $\log[Z/X] \approx [Fe/H] + \log[Z/X]_{\odot}$ and $[Z/X]_{\odot} = 0.0230$ (Grevesse and Sauval, 1998), for the solar mixture. So we can deduce the $[Z/X]_s = 0.0183 - 0.0290$.

All non-asteroseismic observational constraints are listed in Table 1.

2.2 Asteroseismic constraints

Solar-like oscillations of 70 Ophiuchi A have been detected by Carrier and Eggenberger (2006) with the HARPS spectrograph. Fourteen individual modes are identified with amplitudes in the range 11 to 14 cm s^{-1} . Although they listed two groups of frequencies by mode identification (see Table 2 in Carrier and Eggenberger, 2006), one group of frequencies with a average large separation $\Delta\nu = 161.7 \mu\text{Hz}$ was suggested to be more reliable than the other with a average large separation $\Delta\nu = 172.2 \mu\text{Hz}$. The star 70 Ophiuchi A is very similar to α Cen B with the same spectral type and similar large separation, which has a mean small separation of $10 \mu\text{Hz}$. It is thought that the small separation should be similar. By inspecting the results of the mode identification, they note that the value of the small separation coming from the identification with the large separation of $172.2 \mu\text{Hz}$ is significantly different from $10 \mu\text{Hz}$. If the large separation is $172.2 \mu\text{Hz}$, the small separation will be lower than $6.5 \mu\text{Hz}$ in the frequency range $3 - 4.5 \text{ mHz}$. Although this identification is less reliable than the one with a large separation of $161.7 \mu\text{Hz}$, the solution $\Delta\nu = 172.2 \mu\text{Hz}$ can not be ruled out definitely. We refer to these two groups of results in the paper and make analyses in Sect. 4 and Sect. 5.

Table 2
Input parameters for model tracks.

Variable	Minimum Value	Maximum Value	δ
Mass M/M_{\odot}	0.85	0.93	0.01
Initial heavy element abundance Z_i	0.017	0.023	0.001
Initial Helium abundance Y_i	0.26	0.30	0.01

Note.—The value δ defines the increment between minimum and maximum parameter values used to create the model array.

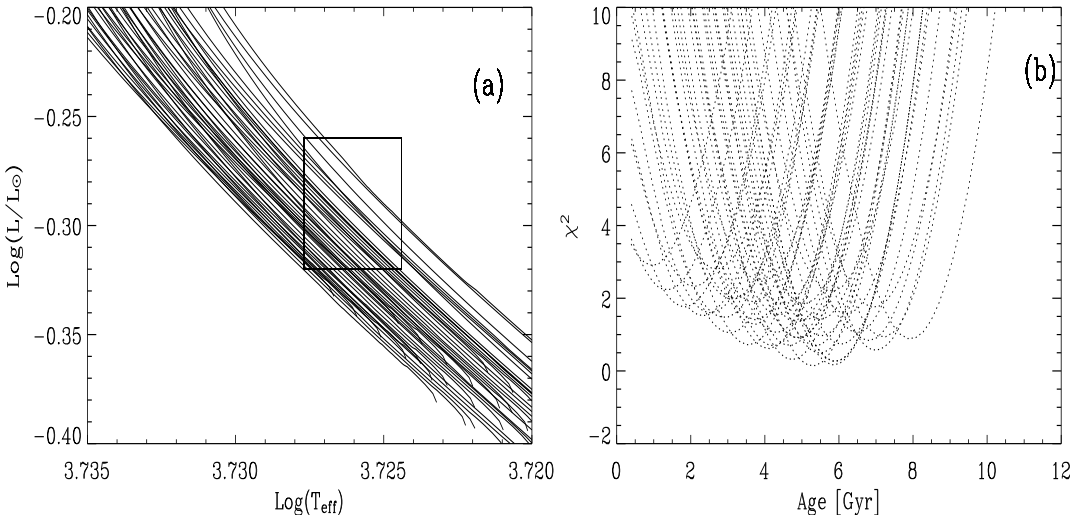


Fig. 1. Evolutionary tracks in the HR diagram and χ^2 as a function of age for 70 Ophiuchi A. a) The selected individual stellar evolutionary tracks (44 in total). b) χ^2 values calculated for 70 Ophiuchi A observational data using different Z_i , Y_i and Mass, plotted as a function of age. χ^2 refers to non-asteroseismological observables as denoted by eq. (1).

3 Stellar models

We will construct a grid of stellar evolutionary models by Yale stellar evolution code (YREC; Guenther et al., 1992) with microscopic diffusion. The initial zero-age main sequence (ZAMS) model used for 70 Ophiuchi A was created from pre-main sequence evolution calculations. In these computations, we do not consider rotation and magnetic field effect. These models are computed using OPAL equation of state tables EOS2001 (Rogers and Nayfonov, 2002), the opacities interpolated between OPAL GN93 (Iglesias and Rogers, 1996) and low temperature tables (Alexander and Ferguson, 1994). Using the standard mixing-length theory, we set $\alpha = 1.7$ for all models, close to the value which is required to reproduce the solar radius under the same physical assumptions and stellar evolution code. Meanwhile, it must be emphasized that there are still a number of uncertainties in our analyses, foremost among which is the still open question of mixing-length theory responsible for the stellar model. The nuclear reaction rates have been updated according

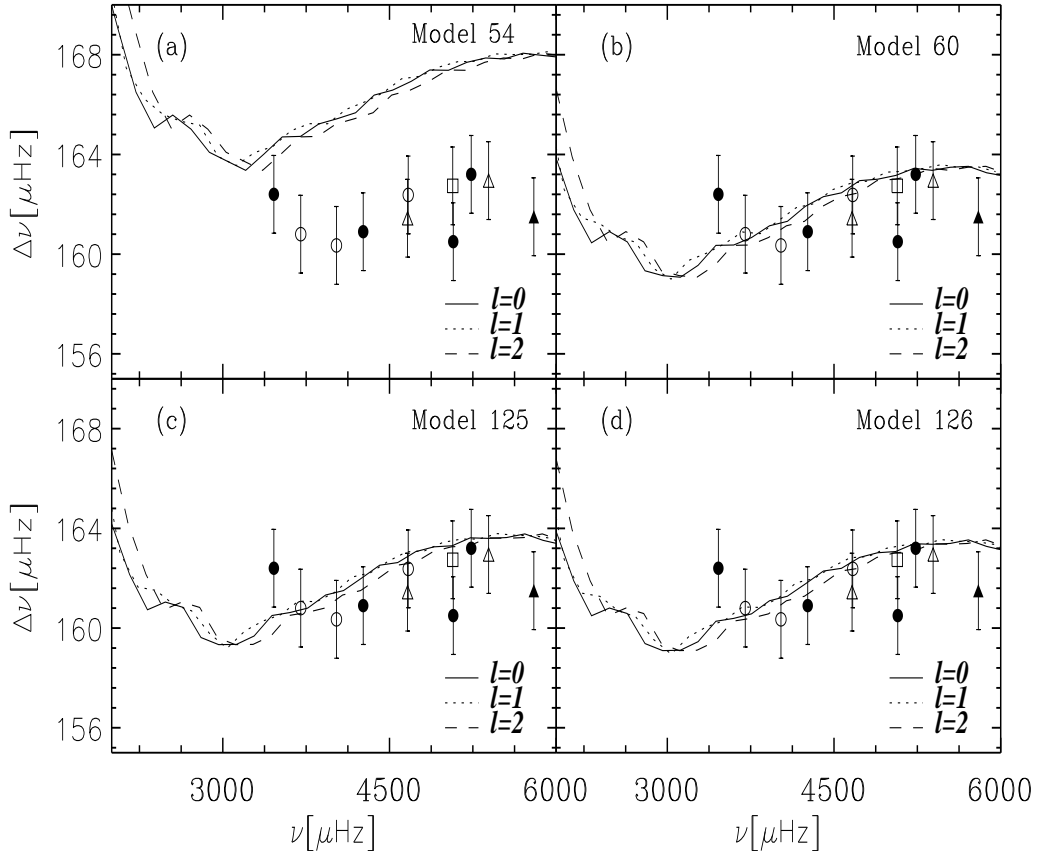


Fig. 2. Large-frequency separations vs. frequency for the Models 54, 60, 125, 126 (in Table 3). The observable large separations $\Delta\nu$ versus frequency for p -modes of degree $l = 0$ (●), $l = 1$ (▲) and $l = 2$ (■) are obtained from Carrier and Eggenberger (2006), which correspond to the average large separation of $161.7 \mu\text{Hz}$. Open symbols correspond to large separation averages taken between non-successive modes and vice versa. All individual errors are fixed to $\sqrt{2} \times 1.1 \mu\text{Hz}$ (half resolution).

to Bahcall and Pinsonneault (1995). The Krishna-Swamy Atmosphere T- τ relation is used for this solar-like star (Guenther and Demarque, 2000). Also, we consider the microscopic diffusion effect, by using the diffusion coefficients of Thoul et al. (1994). Since 70 Ophiuchi A, like α Cen B, is less massive than the Sun, the mass contained in its convective zone is much larger and, therefore, the effect of microscopic diffusion is much smaller (Miglio and Montalbán, 2005; Morel and Baglin, 1999). However, it is necessary to consider this effect as physical process in stellar modeling (see Provost et al., 2005, 2006).

In general, the determination of parameters (M, t, Y_i, Z_i) fitting the observational constraints needs two steps. The first step is to construct a grid of models with position in the HR diagram in agreement with the observational values of the luminosity, the effective temperature and the surface metallicity. The principal constraints deduced from non-asteroseismic observation are listed in Table 1. The error

box, which is composed of observational effective temperature and luminosity, represents the possible position of 70 Ophiuchi A in the HR diagram (see Fig. 1a). According to the results of Fernandes et al. (1998), we list the parameter space of mass M , the initial heavy-element abundance Z_i and the initial helium abundance Y_i in Table 2. Since the microscopic diffusion is included in our paper, we give the wider parameter space of initial heavy-element abundance Z_i than the range of Z_i of Fernandes et al. (1998).

By adjusting three parameters M , Y_i and Z_i listed in Table 2, we can obtain many evolutionary tracks passing through the error box in the HR diagram. Now we consider a function which describes the agreement between the observations and the theoretical results:

$$\chi^2 \equiv \sum_{i=1}^3 \left(\frac{C_i^{theo} - C_i^{obs}}{\sigma C_i^{obs}} \right)^2, \quad (1)$$

where \mathbf{C} represent the following quantities: L/L_\odot , T_{eff} and $[Z/X]_s$, \mathbf{C}^{theo} represent the theoretical values and \mathbf{C}^{obs} represent the observational values listed in Table 1. The vector $\sigma \mathbf{C}_i^{obs}$ contains the errors on these observations which are also given in Table 1.

As Fernandes(1998) has pointed that the age of 70 Ophiuchi A is 3 ± 2 Gyr, it is reasonable for us to choose the evolutionary tracks passing through the error box within 8 Gyr. We select 44 evolutionary tracks passing through error box as our possible candidates to go on with our investigations. Fig. 1a gives 44 evolutionary tracks, and Fig. 1b presents χ^2 as a function of the age correspondingly. It is well-known that χ^2 is smaller, the more competitive is the candidate. Fig. 1b shows that models with χ^2 smaller than 1 have ages between 3Gyr to 7Gyr. From Fig. 1a, we find that the upper section of error box is empty. The reason of the empty upper section of the error box is related to the range of initial parameters, like mass, initial composition and specially the mixing length parameter. We think that the future interferometric measurement of the radius could reduce the domain of the possible position in the HR diagram (e.g., Provost et al., 2006).

The second step is to determine the optimum model using the asteroseismic measurements. We will select a grid of models along these 44 tracks shown in Fig. 1a to calculate the low- l p -modes frequencies. We list the representative models extracted from every tracks in Table 3.

The detailed pulsation analysis is described in the next section.

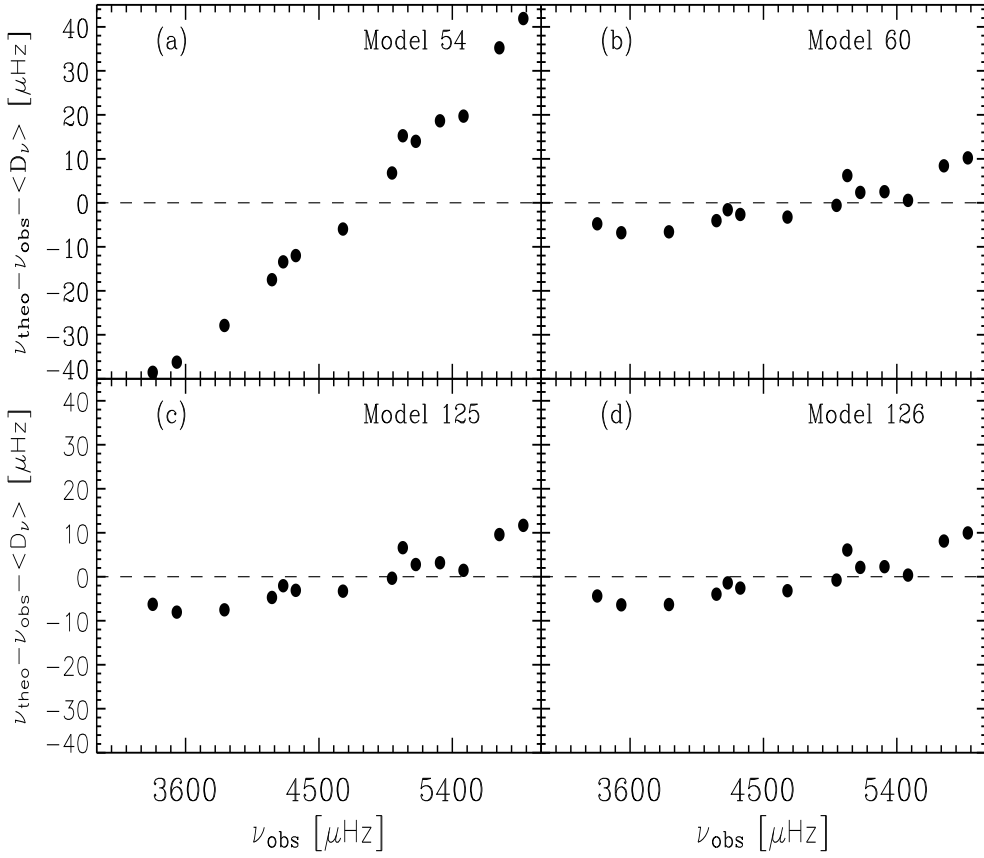


Fig. 3. Differences between calculated and observable frequencies for the Model 54, 60, 125, 126 in Table 3. The systematic shifts $\langle D_\nu \rangle$ for the four models are 30.059, 63.75, 70.252, 63.24 μHz , respectively. The observable frequencies correspond to the average large separation of 161.7 μHz (see text for details).

4 Pulsation analysis

4.1 Selecting the optimum model

Using Guenther's pulsation code (Guenther, 1994), we calculate the adiabatic low- l p -mode frequencies of the selected models. We define the large separations $\Delta\nu$ and small separations $\delta\nu$ in the usual way (Tassoul, 1980):

$$\Delta\nu_{n,l} \equiv \nu_{n,l} - \nu_{n-1,l} \quad (2)$$

and

$$\delta\nu_{n,l} \equiv \nu_{n,l} - \nu_{n-1,l+2}, \quad (3)$$

where n is the radial order, l is the degree, and ν is the frequency. Because the expected acoustic cutoff has a limit, we only calculate the mean large- and small-separations by averaging over $n = 10 - 30$ (See Murphy et al., 2004). Within these

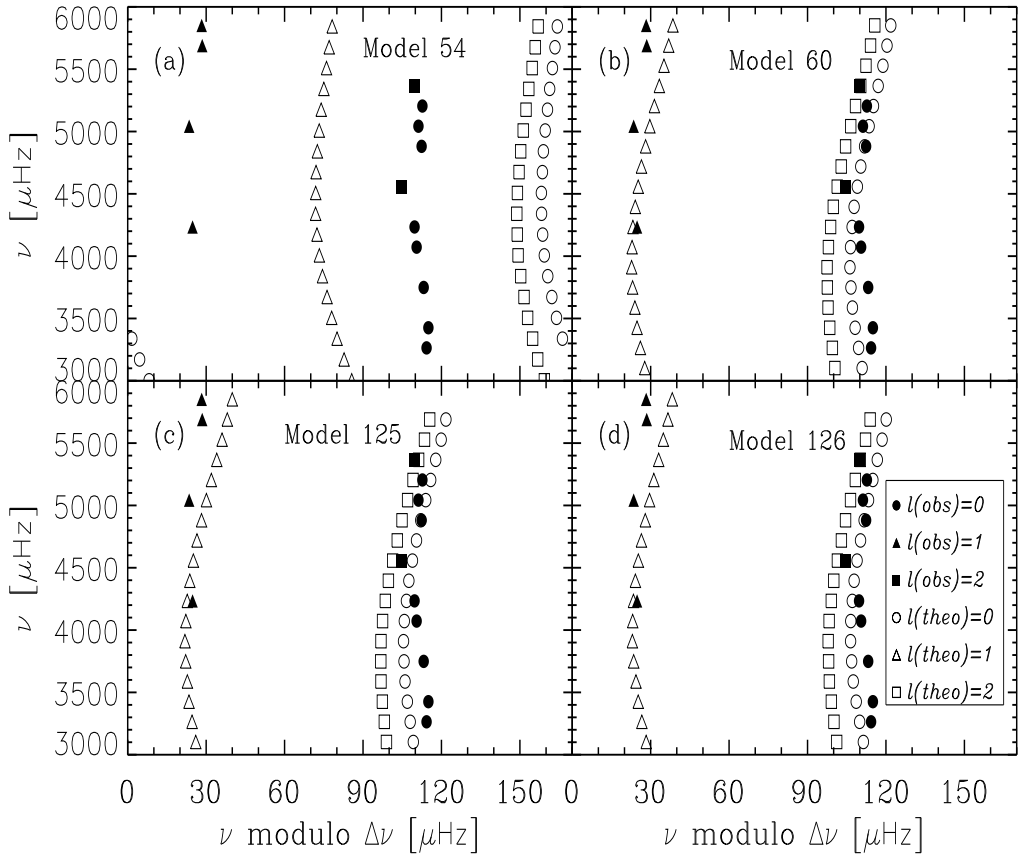


Fig. 4. Echelle diagrams for the Models 54, 60, 125, 126 (in Table 3), which average large separations $\langle \Delta\nu \rangle$ are 166.22, 161.7, 161.92, 161.68 μHz , respectively. The systematic shift $\langle D_\nu \rangle$, which have been applied to the theoretical frequencies, are 30.059, 63.75, 70.252, 63.24 μHz , for the four models respectively. Open symbols refer to the theoretical frequencies, and filled symbols to the observable frequencies. Circles are used for $l = 0$ modes, triangles for $l = 1$ modes, and squares for $l = 2$ modes. The observable frequencies correspond to the average large separation of 161.7 μHz (see text for details).

44 tracks, we list 129 models in Table 3. $\langle \Delta\nu_l \rangle$ represents the mean of large separations $\Delta\nu_{n,l}$ for $n = 10$ to 30. The frequency range corresponds to about 2000 μHz –6000 μHz . Additionally, $\langle \Delta\nu \rangle$ represents the mean of $\langle \Delta\nu_l \rangle$ for $l = 0$ to 3. In the same way, $\langle \delta\nu_{02} \rangle$ and $\langle \delta\nu_{13} \rangle$ represent the mean of $\delta\nu_{n,0}$ and $\delta\nu_{n,1}$ for $n = 10$ to 30, respectively. So far, we only know the large separations and the fourteen individual modes of the star based on the asteroseismic data of Carrier and Eggenberger (2006). Guenther (1998) pointed that the large separations are most easily identifiable characteristics in the p -mode spectrum. Because they are seen as a peak in the Fourier transform of the power spectrum and they are mostly uncontaminated by composition effects, these large separations provide an efficient way to constrain stellar model. It is also important to remember that the theoretical frequencies calculated in our paper should not be expected to match the observed frequencies of Carrier and Eggenberger (2006) perfectly. We think that there are

three reasons. Firstly, our theoretical models do not match the mass and radius of the star precisely. Secondly, the uncertainty in calculating the sound speed in the outer layers of the models comes into being, where non-adiabatic effects become important. Thirdly, at high frequencies, the effect of the convection-oscillation interactions is larger and the description of convection is open problem. Although the differences between the theoretical frequencies and the observed frequencies could result in significant effect on the large separations, we think that the effect is small due to the large separations correspond to differences between frequencies of modes with the same angular degree l and consecutive radial order n . Therefore, in our paper, we think that the matching the observable large separations is the important criterion to select the optimum model. In Table 3, we find that the average large separations of Model 60, Model 125 and Model 126 are 161.7, 161.92 and 161.68 μHz , in good agreement with the mean value derived from Carrier and Eggenberger (2006). So we can tentatively say that these models may be the best fit models. In Fig. 2, we plot the observational results about the large separations and the errors. Also we plot the large separation as a function of frequency for Model 54 in Fig. 2a, Model 60 in Fig. 2b, Model 125 in Fig. 2c and Model 126 in Fig. 2d. We clearly find that the theoretical large separations of the Model 60, Model 125 and Model 126 are consistent with the observations. Model 54, as the representative of many non-fit models, is not consistent with the observational large separations. Therefore, we have sufficient reasons to say that Model 60, Model 125 and Model 126 are really the best fit models. Meanwhile, we can predict that the radius of star is $0.860 - 0.865 R_\odot$ and the age is about 6.8 – 7.0 Gyr with mass $0.89 - 0.90 M_\odot$ presently.

Once the asteroseismic observation can confirm the large separations to be $161.7 \pm 0.3 \mu\text{Hz}$ and the theory Model 60, Model 125, Model 126 are considered as the best models, we can predict that the mean small separation $\langle \delta\nu_{02} \rangle$ is about $10.29 - 10.48 \mu\text{Hz}$ and the radius of the star is about $0.860 - 0.865 R_\odot$. Direct measurements of stellar diameters from interferometric observations should provide an independent check for asteroseismic predictions such as Kervella et al. (2003a, 2003b).

In order to compare the theoretical p -mode frequencies deduced from the models in Table 3 with the observational frequencies provided by Carrier and Eggenberger (2006), we plot the echelle diagram of every model and find that no model can fit observational frequencies. For the exact values of the frequencies, considering above three reasons, a linear shift of a few μHz between theoretical and observational frequencies is perfectly acceptable. Taking into account it, we define the mean value of the difference between the theoretical and observational frequencies (e.g., Eggenberger et al., 2004b, 2005):

$$\langle D_\nu \rangle \equiv \frac{1}{N} \sum_{i=1}^N (\nu_i^{theo} - \nu_i^{obs}). \quad (4)$$

where N is the number of observable frequencies ($N = 14$).

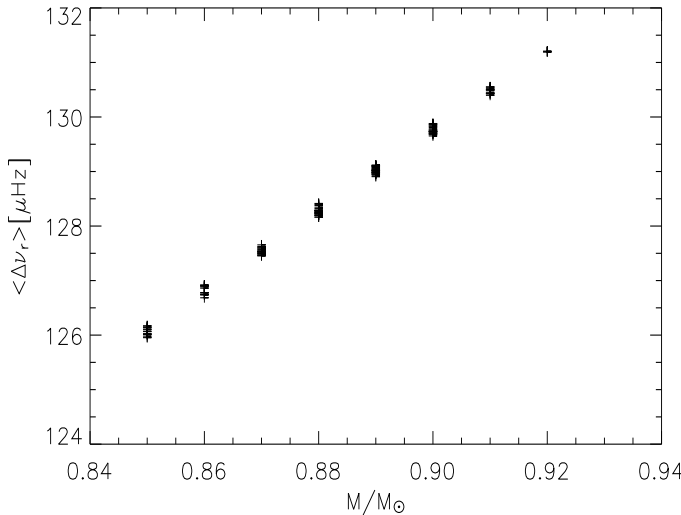


Fig. 5. The “reduced” large separation vs. mass for each of the 129 stellar models.

Taking into account the systematic difference $\langle D_\nu \rangle$ between theoretical and observable frequencies, we plot the differences between calculated and observed frequencies in Fig. 3 and the echelle diagram in Fig. 4. The observable frequencies correspond to the average large separation of $161.7 \mu\text{Hz}$ in these figures. Fig. 3a, Fig. 3b, Fig. 3c and Fig. 3d correspond to the Model 54 with $\langle D_\nu \rangle = 30.059 \mu\text{Hz}$, Model 60 with $\langle D_\nu \rangle = 63.75 \mu\text{Hz}$, Model 125 with $\langle D_\nu \rangle = 70.252 \mu\text{Hz}$, and Model 126 with $\langle D_\nu \rangle = 63.24 \mu\text{Hz}$, respectively. Fig. 4a, Fig. 4b, Fig. 4c and Fig. 4d show the echelle diagram of the Model 54, Model 60, Model 125 and Model 126 respectively. For p -modes in the asymptotic theory ($n \gg l$), the large separations are nearly constant; meanwhile the so-called “echelle diagrams” present the frequencies in ordinates, and the same frequencies modulo the average large separation in abscissa. So the asymptotic theory predicts an approximated vertical line for given degree. In this case, Fig. 4b, Fig. 4c and Fig. 4d show that the theoretical frequencies of Model 60, Model 125, Model 126 can fit the observable frequencies with $161.7 \mu\text{Hz}$. Meanwhile, we find that the systematic differences $\langle D_\nu \rangle$ are larger than the results of α Cen B obtained by Eggenberger (2004b). It is interesting to analyze the difference in future work.

4.2 Asymptotic formula and frequency analysis

4.2.1 Large Separations and Small Separations

It is well known from asymptotic theory that the large separations are mainly sensitive to the stellar radius (Tassoul, 1980; Christensen-Dalsgaard, 1984). More precisely, the asymptotic behavior of $\Delta\nu$ is expected to scale with $(M/R^3)^{1/2}$, where M is the mass of the star and R is its radius. Meanwhile, Murphy et al. (2004) find that a degeneracy in predicted radius occurs for models of different mass. Here, the

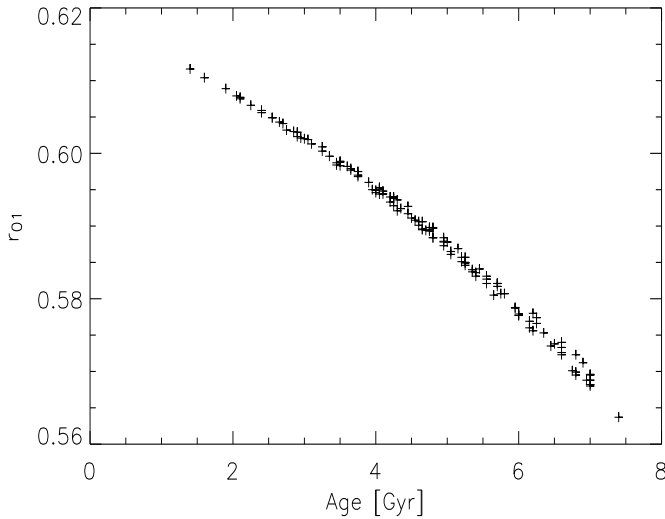


Fig. 6. The ratio of small separations adjacent in l vs. age for each of 129 stellar models.

degeneracy means that the $\langle \Delta\nu \rangle$ changes with radius and mass (see Fig. 4 in Murphy et al., 2004). In order to lift the degeneracy, Fernandes and Monteiro (2003) and Murphy et al. (2004) assumed homology to compare theoretical models by introducing a “reduced” radius, such as

$$\langle \Delta\nu_r \rangle = \langle \Delta\nu_{n,l} \rangle (R/R_\odot)^{3/2}. \quad (5)$$

Here, we name the quantity $\langle \Delta\nu_r \rangle$ “reduced” large separation. We draw the “reduced” large separation $\langle \Delta\nu_r \rangle$ versus mass in Fig. 5 and list the values of $\langle \Delta\nu_r \rangle$ for each model in Table 3. From Fig. 5, we find that the degeneracy was lifted approximately. It is easily seen that the values of the $\langle \Delta\nu_r \rangle$ are relatively consistent with each mass. It is successful using the $\langle \Delta\nu_r \rangle$ instead of large separations to indicate the stellar mass.

The small separations, like the large separations, will be visible as peaks in the Fourier transform of the power spectrum. At the earlier stage, Christensen-Dalsgaard (1984) proposed that the calculation of small separations could put a constraint on the age the star. Subsequently, Ulrich (1986) realized that only if the composition of the star is known completely can one use the small separations to correctly identify a stellar age. This point has been illustrated in Murphy et al. (2004). Thus, the various chemical compositions create a degeneracy in age determination (see Murphy et al., 2004). Namely, the small separations $\delta\nu$ change with the initial composition and age. In the next section, we will discuss this problem and propose a quantity which may be correlated with stellar age.

4.2.2 A new quantity be proposed

At the present time, we can know the stellar internal structure and understand the stellar evolution from oscillation frequencies. Thus asteroseismology provides a

window to “see” the interior of star. But the observation of solar-like oscillation is very difficult because of their small amplitude. So far, we only obtain the knowledge of the stellar interior from the limited modes ($l = 0, 1, 2, 3$) which can be observed. Many authors proposed some quantity as diagnostic purposes to probe the stellar internal and constraint the model parameters (Christensen-Dalsgaard, 1984, 1988, 1993; Ulrich, 1986, 1988; Gough, 1987, 1990a, 2003). For p -modes of solar-like stars, the usual frequency separations are the large separation defined by equation (2) and the small separation defined by equation (3). Additionally, Roxburgh (1993) and Roxburgh and Vorontsov (2003) considered the following separations:

$$\delta_{01}(n) = \frac{1}{8}(\nu_{n-1,0} - 4\nu_{n-1,1} + 6\nu_{n,0} - 4\nu_{n,1} + \nu_{n+1,0}), \quad (6)$$

$$\delta_{10}(n) = -\frac{1}{8}(\nu_{n-1,1} - 4\nu_{n-1,0} + 6\nu_{n,1} - 4\nu_{n+1,0} + \nu_{n+1,1}), \quad (7)$$

and defined the ratios d_{ij} of small to large separations as follows:

$$\begin{aligned} d_{02}(n) &= \frac{\delta\nu_{02}(n)}{\Delta\nu_1(n)}, & d_{13}(n) &= \frac{\delta\nu_{13}(n)}{\Delta\nu_0(n+1)}, \\ d_{01}(n) &= \frac{\delta\nu_{01}(n)}{\Delta\nu_1(n)}, & d_{10}(n) &= \frac{\delta\nu_{10}(n)}{\Delta\nu_0(n+1)}. \end{aligned} \quad (8)$$

The ratios d_{ij} of small to large separations are independent of the structure of the outer layers of a star, and therefore provide a diagnostic of the stellar interior alone.

In addition, Gough (1990a), Monteiro and Thompson (1998), Vauclair and Théado (2004), Houdek and Gough (2007a) gave the second differences $\Delta_2\nu_l(n)$:

$$\Delta_2\nu_l(n) = \nu_{n+1,l} + \nu_{n-1,l} - 2\nu_{n,l}. \quad (9)$$

The second differences $\Delta_2\nu_l(n)$ can be used to reveal the variation of the first adiabatic exponent γ_1 dependent of the influence of the ionization of helium on the low-degree acoustic oscillation frequencies in model of solar-type stars. Recently, Houdek and Gough (2007b) stated that the second differences can provide a measure of helium abundance and hence precisely lift the degeneracy between composition and age.

Summarizing the above character separation, we find that investigation of lifting the degeneracy between the chemical compositions and the age is interesting. We begin with our investigation from a well-known asymptotic formula.

The asymptotic formula for the frequency $\nu_{n,l}$ of a stellar p -mode of order n and degree l was given by Tassoul (1980):

$$\nu_{n,l} \simeq (n + \frac{l}{2} + \epsilon)\nu_0 - [Al(l+1) - B]\nu_0^2\nu_{n,l}^{-1}, \quad (10)$$

where, the characteristic ν_0 is related to the run of sound travel time across the stellar diameter; A is a measure of the sound-speed gradient and most sensitive to conditions in the stellar core (see Gough and Novotny, 1990b; Gough, 2003; Christensen-Dalsgaard, 1993; Guenther and Brown, 2004), ϵ and B are constants which are the functions of the equilibrium model. It should be noted that the classical asymptotic theory of Tassoul (1980), although providing good results at the first order in frequency, does not represent with accuracy the p -mode spectrum of the stars considered. Several authors (e.g., Gabriel, 1989; Audard and Provost, 1994; Roxburgh and Vorontsov, 2000a, 2000b, 2001) have been discussed the difficulties of the asymptotic theory, particularly for evolved models with rapid variation in the sound speed in the core.

Using the equation (2) and the asymptotic formula (10), the large separation can be written as follows (Gough and Novotny, 1990b):

$$\begin{aligned}\Delta\nu_{n,l} &= \nu_{n,l} - \nu_{n-1,l} \\ &= \nu_0 - [Al(l+1) - B]\nu_0^2 \frac{\nu_{n-1,l} - \nu_{n,l}}{\nu_{n,l} \cdot \nu_{n-1,l}},\end{aligned}\quad (11)$$

Taking the first order of $\nu_{n,l}$ for the $n \gg l$ approximately, we can obtain the result like Gough and Novotny (1990b) and equation (11) becomes:,

$$\begin{aligned}\Delta\nu_{n,l} &\approx \nu_0 \left[1 - \frac{Al(l+1) - B}{(n + \frac{l}{2} + \epsilon)(n - 1 + \frac{l}{2} + \epsilon)} \right]^{-1} \\ &\approx \nu_0.\end{aligned}\quad (12)$$

Using the same approximate method, we can obtain the expression of small separation:

$$\delta\nu_{n,l} = \delta\nu_{l,l+2} \approx \frac{(4l+6)\nu_0 A}{n + \frac{l}{2} + \epsilon}. \quad (13)$$

Due to the small separations are rather sensitive to composition and therefore to the structure of the core, especially the extreme sensitivity of the stellar core density stratification to several parameters (Guenther and Demarque, 2000; Morel et al., 2000), we define another quantity about the ratio of average small separation adjacent in l :

$$r_{01} = \frac{\langle \delta\nu_{0,2} \rangle}{\langle \delta\nu_{1,3} \rangle}. \quad (14)$$

Using the equation (14), we calculate the values of r_{01} and list it in table 3. Based on the results of numerical calculations, we plot the ratio r_{01} versus age in Fig. 6.

Fortunately, we find that the ratio r_{01} is tightly correlated with age and decreases monotonously with age. We think that the likely reason comes from the perturbation to the gravitational potential, neglected in the asymptotic relation (10), which affects modes of the lowest degrees most strongly and which probably increases with evolution due to the increasing central density. These effects are most important for modes of the lowest degrees which penetrate most deeply and hence affect $\delta\nu_{0,2}$ more than $\delta\nu_{1,3}$, leading to the dependence of r_{01} on age.

From the Fig. 6, the values of $r_{0,1}$ in table 3 and the above discussion, we can conclude that this quantity r_{01} can lift the degeneracy between the chemical compositions and age. The analysis was inspired by Fernandes and Monteiro (2003) and Murphy et al. (2004). So, we can obtain the r_{01} which may indicate stellar age, if we consider a frequency ratio. As illustrated in Fig. 6, the quantity r_{01} is tightly correlate with stellar age over a substantial range of the remaining parameters, including composition. At the same time, we need to point out that the range of variation of this quantity is relatively modest, compared to likely observational errors. Also, it is clear that the present data for 70 Ophiuchi A are not adequate to evaluate this quantity. We think that using this quantity to evaluate the stellar age will be convenient based on asteroseismic data which will be provided in the future.

5 Discussion and conclusions

The models of 70 Ophiuchi A are obtained by fitting effective temperature, luminosity, surface metallicity and asteroseismic observations.

We list a series of possible models in Table 3. So far, we think that Model 60, Model 125 and Model 126 are the best models. With the advance in observation, the precise asteroseismic data will provide more strict constraints on theoretical models. The conclusions of the paper are:

1. Using the latest asteroseismic observation, we try our best to construct the best model of 70 Ophiuchi A. So far, we only select the Model 60, Model 125 and Model 126, which can be fit for the observation, as the optimum models. These models are correspond to the radius of this star is about $0.860 - 0.865 R_\odot$ and the age is about $6.8 - 7.0$ Gyr with mass $0.89 - 0.90 M_\odot$.
2. By calculating many theoretical models, we want to use the theoretical frequencies to compare with observational frequencies and help to definitely validate the observational data.
3. We obtain a new quantity r_{01} which can lift the degeneracy between the initial compositions and the stellar age. By calculation, we prove that it can be valuable for the indication of the stellar age.

4. Important point is that we test our stellar structure and evolution theory. Meanwhile we find the confrontation of observations and theoretical models. Actually we have neglect some important effects, such as rotation and magnetic field, which can impact on the internal structure and evolution. Thus, the theory models which we have constructed can not fit observation perfectly. The detailed comparisons of individual mode frequencies will also require taking into account the effects of turbulence in the outer convective unstable layers in the stellar models, which shift the observed frequencies. The parameterization of turbulence tested on the Sun by Li et al. (2002) can be applied to models for solar-like stars as well. This parameterization can be extended to other stars by using the three-dimensional radiative hydrodynamic simulations of Robinson et al. (2003), which are based on the same microscopic physics and can readily be parameterized in the YREC stellar evolution code.

Acknowledgements

We are grateful to anonymous referees for their constructive suggestions and valuable remarks to improve the manuscript. This work was supported by The Ministry of Science and Technology of the People's republic of China through grant 2007CB815406, and by NSFC grants 10173021, 10433030, 10773003, and 10778601.

References

- Alexander, D. R., Ferguson, J. W., 1994. ApJ 437, 879.
- Audard, N., Provost, J., 1994. A&A 282, 73.
- Bahcall, J. N., Pinsonneault, M. H., Wasserburg, G. J., 1995. RvMP 67, 781.
- Batten, A. H., Fletcher, J. M., Campbell, B., 1984. PASP 96, 903.
- Bedding, T. R., Butler, R. P., Kjeldsen, H., Baldry, I. K., O'Toole, S. J., Tinney, C. G., Marcy, G. W., Kienzle, F., Carrier, F., 2001. ApJ 549, L105.
- Bedding, T. R., Kjeldsen, H.; Butler, R. P., McCarthy, C., Marcy, G. W., O'Toole, S. J., Tinney, C. G., Wright, J. T., 2004. ApJ 614, 380.
- Bouchy, F., Carrier, F., 2002. A&A 390, 205.
- Bouchy, F., Bazot, M., Santos, N. C., Vauclair, S., Sosnowska, D., 2005. A&A 440, 609.
- Carrier, F., Bouchy, F., Kienzle, F., Bedding, T. R., Kjeldsen, H., Butler, R. P., Baldry, I. K., O'Toole, S. J., Tinney, C. G., Marcy, G. W., 2001. A&A 378, 142.
- Carrier, F., Bourban, G., 2003a. A&A 406, L23.

- Carrier, F., Bouchy, F., Eggenberger, P., 2003b. In Thompson, M. J., Cunha, M. S., & Monteiro, M. J. P. F. G., editors, Asteroseismology Across the HR Diagram, page P311. Kluwer.
- Carrier, F., Eggenberger, P., Bouchy, F., 2005a. A&A 434, 1085.
- Carrier, F., Eggenberger, P., DAlessandro, A., Weber, L., 2005b. NewA 10, 315.
- Carrier, F., Eggenberger, P., 2006. A&A 450, 695.
- Christensen-Dalsgaard, J., 1984. in Mangeney A., Praderie, F., eds, Space Research Prospects in Stellar Activity and Variability, Paris Observatory Press, Paris, P11.
- Christensen-Dalsgaard, J., 1988. in Advances in Helio and Asteroseismology, ed. J. Christensen-Dalsgaard, & S. Frandsen(Reidel), 295.
- Christensen-Dalsgaard, J., 1993. in Seismic Investigation of the Sun and Stars, ed. T. M. Bron, A.S.P. Conf. Ser 42, 347.
- Eggenberger, P., Carrier, F., Bouchy, F., Blecha, A., 2004a. A&A 422, 247.
- Eggenberger, P., Charbonnel, C., Talon, S., Meynet, G., Maeder, A., Carrier, F., Bourban, G., 2004b. A&A 417, 235.
- Eggenberger, P., Carrier, F., Bouchy, F., 2005. NewA 10, 195.
- Fernandes, J., Lebreton, Y., Baglin, A., Morel, P., 1998. A&A 338, 455.
- Fernandes, J., Monteiro, M. J. P. G., 2003. A&A 399, 243.
- Gabriel, M., 1989. A&A 226, 278.
- Gough, D. O., 1987. Nature 326, 257.
- Gough, D. O., 1990a. in Progress of Seismology of the Sun and Stars, Proc. Oji International Seminar Hakone (Japan: Springer Verlag), Lect. Notes Phys., 367, 283.
- Gough, D. O., Novotny, E., 1990b. SoPh 128, 143.
- Gough, D. O., 2003. Ap&SS 284, 165.
- Grevesse. N., Sauval, A. J., 1998. SSRv 85, 161.
- Gray, D. H., Johanson, H., 1991. PASP 103, 439.
- Guenther, D. B., Demarque, P., Kim, Y.-C., Pinsonneault, M. H., 1992. ApJ 387, 372.

- Guenther, D. B., 1994. *ApJ* 422, 400.
- Guenther, D. B., 1998. in Proc. SOHO 6/GONG 98 Workshop, Structure and Dynamics of the Interior of the Sun and Sun-like Stars, ed S. Korzennik & A. Wilson (ESA SP-418), 375.
- Guenther, D. B., Demarque, P., 2000. *ApJ* 531, 503.
- Guenther, D. B., Brown, K. I. T., 2004. *ApJ* 600, 419.
- Heintz, W. D., 1988. *JRASC* 82, 140.
- Houdek, G., Gough, D. O., 2007a. *MNRAS* 375, 861.
- Houdek, G., Gough, D. O., 2007b. *AIPC* 984, 219.
- Iglesias, C. A., Rogers, F. J., 1996. *ApJ* 464, 943.
- Kervella, P., Thévenin, F., Morel, P., Bordé, P., Di Folco, E., 2003a. *A&A* 408, 681.
- Kervella, P., Thévenin, F., Ságransan, D., Berthomieu, G., Lopez, B., Morel, P., Provost, J., 2003b. *A&A* 404, 1087.
- Kervella, P., Thévenin, F., Morel, P., Berthomieu, G., Bordé, P., Provost, J., 2004. *A&A* 413, 251.
- Kjeldsen, H., Bedding, T. R., Baldry, I. K., Brunett, H., Butler, R. P., Fischer, D. A., Frandsen, S., Gates, E. L., Grundahl, F., Lang, K., Marcy, G. W., Misch, A., Vogt, S. S., 2003. *AJ* 126, 1483.
- Kjeldsen, H., Bedding, T. R., Butler, R. P., Christensen-Dalsgaard, J., Kiss, L. L., McCarthy, C., Marcy, G. W., Tinney, C. G., Wright, J. T., 2005. *ApJ* 635, 1281.
- Li, L. H., Robinson, F. J., Demarque, P., Sofia, S., Guenther, D. B., 2002. *ApJ* 567, 1192.
- Martić, M., Lebrun, J.-C., Appourchaux, T., Korzennik, S. G., 2004a. *A&A* 418, 295.
- Martić, M., Lebrun, J. C., Appourchaux, T., Schmitt, J., 2004b. In Danesy, D., editor, SOHO 14/GONG 2004 Workshop, Helio- and Asteroseismology: Towards a Golden Future, ESA SP-559, page 563.
- Miglio, A., Montalbán, J., 2005. *A&A* 441, 615.
- Monteiro, M. J. P. F. G., Thompson, M. J., 1998. in New Eyes to See Inside the Sun and Stars (Dordrecht: Kluwer), ed. F. L. Deubner, J. Christensen-Dalsgaard, & D.

- W. Kurtz, Proc. IAU Symp., 185, 317.
- Morel, P., 1997. A&AS 124, 597.
- Morel, P., Baglin, A., 1999. A&A 345, 156.
- Morel, P., Provost, J., Lebreton, Y., Thévenin, F., Berthomieu, G., 2000. A&A 363, 675.
- Mosser, B., Bouchy, F., Catala, C., Michel, E., Samadi, R., Thévenin, F., Eggenberger, P., Sosnowska, D., Moutou, C., Baglin, A., 2005. A&A 431, L13.
- Murphy, E. J., Demarque, P., Guenther, D. B., 2004. ApJ 605, 472.
- Perrin, M. N., Cayrel, de S. G., Cayrel, R., 1975. A&A 39, 97.
- Peterson, R., 1978. ApJ 224, 595.
- Pourbaix, D., 2000. A&AS 145, 215.
- Provost, J., Martic, M., Berthomieu, G., 2004. ESA SP. 559, 594.
- Provost, J., Berthomieu, G., Bigot, L., Morel, P., 2005. A&A 432, 225.
- Provost, J., Berthomieu, G., Martić, M., Morel, P., 2006. A&A 460, 759.
- Robinson, F. J., Demarque, P., Li, L. H., Sofia, S., Kim, Y.-C., Chan, K. L., Guenther, D. B., 2003. MNRAS 340, 923.
- Rogers, F. J., Nayfonov, A., 2002. ApJ 576, 1064.
- Roxburgh, I. W., 1993. in PRISMA, Report of Phase A Study, ed. T. Approurchaux, et al., ESA 93, 31.
- Roxburgh, I. W., Vorontsov, S. V., 2000a. MNRAS 317, 141.
- Roxburgh, I. W., Vorontsov, S. V., 2000b. MNRAS 317, 151.
- Roxburgh, I. W., Vorontsov, S. V., 2001. MNRAS 322, 85.
- Roxburgh, I. W., Vorontsov, S. V., 2003. A&A 411, 215.
- Tassoul, M., 1980. ApJS 43, 469.
- Thoul, A. A., Bahcall, J. N., Loeb, A., 1994. ApJ 421, 828.
- Thévenin, F., Provost, J., Morel, P., Berthomieu, G., Bouchy, F., Carrier, F., 2002. A&A 392, 9.

Ulrich, R. K., 1986. ApJ 306, L37.

Ulrich, R. K., 1988. IAUS 123, 299.

Vauclair, S., Théado, S., 2004. A&A 425, 179.

Online Material

Table 3

Model parameters (M: mass; Y_i : initial Helium abundance; Z_i : initial heavy element abundance; $\log T_{eff}$: log-effective temperature; $\log L$: log-luminosity; R: radius; $\langle \Delta v_l \rangle$: $\frac{1}{21} \sum_{n=10}^{30} \Delta v_{n,l}$; $\langle \Delta v \rangle$: $\frac{1}{4} \sum_{l=0}^3 \langle \Delta v_l \rangle$; $\langle \delta v_{02} \rangle$: $\frac{1}{21} \sum_{n=10}^{30} \delta v_{n,0}$; $\langle \delta v_{13} \rangle$: $\frac{1}{21} \sum_{n=10}^{30} \delta v_{n,1}$; r_{01} : $\frac{\langle \delta v_{02} \rangle}{\langle \delta v_{13} \rangle}$).

Model	M			log L			R			Age						r_{01}
	(M_\odot)	Y_i	Z_i	$\log T_{eff}$	(L_\odot)	(R_\odot)	(Gyr)	$\langle \Delta v_0 \rangle$	$\langle \Delta v_1 \rangle$	$\langle \Delta v_2 \rangle$	$\langle \Delta v_3 \rangle$	$\langle \Delta v \rangle$	$\langle \delta v_{02} \rangle$	$\langle \delta v_{13} \rangle$	$\langle \Delta v_r \rangle$	
1.....	0.85	0.27	0.017	3.7263	-0.319	0.8155	5.15	170.84	170.91	171.06	171.40	171.05	12.46	21.23	125.9677	0.5869
2.....	0.85	0.27	0.017	3.7270	-0.310	0.8215	5.55	168.81	169.07	169.22	169.56	169.16	12.04	20.65	125.9532	0.5831
3.....	0.85	0.27	0.017	3.7276	-0.301	0.8277	5.95	167.11	167.19	167.34	167.68	167.33	11.61	20.06	126.0037	0.5788
4.....	0.85	0.28	0.019	3.7271	-0.319	0.8125	5.05	171.86	171.93	172.07	172.41	172.06	12.48	21.28	126.0129	0.5865
5.....	0.85	0.28	0.019	3.7276	-0.312	0.8170	5.35	170.46	170.53	170.67	171.01	170.66	12.17	20.84	126.0274	0.5840
6.....	0.86	0.27	0.017	3.7277	-0.319	0.8104	3.90	173.46	173.50	173.65	173.99	173.65	13.50	22.65	126.6846	0.5960
7.....	0.86	0.27	0.018	3.7265	-0.319	0.8150	4.60	172.05	172.11	172.26	172.60	172.25	12.87	21.79	126.7347	0.5906
8.....	0.86	0.27	0.018	3.7271	-0.311	0.8201	4.95	170.46	170.52	170.67	171.01	170.66	12.51	21.28	126.7453	0.5879
9.....	0.86	0.27	0.018	3.7276	-0.304	0.8246	5.25	169.07	169.14	169.28	169.62	169.27	12.19	20.84	126.7491	0.5849
10....	0.86	0.28	0.020	3.7273	-0.319	0.8119	4.50	173.11	173.16	173.30	173.63	173.30	12.91	21.84	126.7805	0.5911
11....	0.86	0.28	0.020	3.7276	-0.315	0.8140	4.65	172.43	172.49	172.63	172.96	172.62	12.75	21.63	126.7733	0.5895
12....	0.87	0.26	0.017	3.7258	-0.319	0.8170	4.10	172.40	172.44	172.59	172.94	172.59	13.30	22.36	127.4526	0.5948
13....	0.87	0.26	0.017	3.7267	-0.307	0.8248	4.65	169.96	170.02	170.17	170.51	170.16	12.74	21.57	127.4619	0.5906
14....	0.87	0.26	0.017	3.7276	-0.295	0.8330	5.20	167.46	167.52	167.67	168.01	167.66	12.17	20.78	127.4668	0.5857
15....	0.87	0.26	0.018	3.7246	-0.319	0.8213	4.80	171.09	171.15	171.29	171.64	171.29	12.69	21.52	127.4925	0.5897
16....	0.87	0.26	0.018	3.7261	-0.300	0.8343	5.70	167.10	167.17	167.32	167.66	167.31	11.78	20.25	127.4986	0.5817
17....	0.87	0.26	0.018	3.7276	-0.279	0.8487	6.60	162.90	163.00	163.13	163.48	163.12	10.84	18.94	127.5377	0.5723
18....	0.87	0.27	0.019	3.7266	-0.319	0.8143	4.05	173.30	173.34	173.49	173.83	173.49	13.30	22.35	127.4827	0.5951
19....	0.87	0.27	0.019	3.7276	-0.306	0.8230	4.65	170.59	170.64	170.79	171.12	170.78	12.67	21.49	127.5078	0.5896
20....	0.87	0.27	0.020	3.7255	-0.319	0.8187	4.75	171.96	172.01	172.15	172.49	172.15	12.68	21.51	127.5247	0.5895
21....	0.87	0.27	0.020	3.7266	-0.304	0.8282	5.40	169.02	169.09	169.22	169.56	169.22	12.01	20.58	127.5424	0.5836
22....	0.87	0.27	0.020	3.7276	-0.290	0.8375	6.00	166.21	166.29	166.42	166.75	166.41	11.38	19.70	127.5430	0.5777
23....	0.87	0.28	0.021	3.7275	-0.319	0.8110	3.95	174.43	174.46	174.61	174.94	174.61	13.34	22.42	127.5265	0.5950
24....	0.87	0.28	0.021	3.7276	-0.318	0.8117	4.00	174.20	174.24	174.38	174.71	174.38	13.29	22.35	127.5234	0.5946
25....	0.88	0.26	0.017	3.7271	-0.319	0.8124	2.90	174.85	174.88	175.04	175.37	175.03	14.30	23.72	128.1644	0.6029
26....	0.88	0.26	0.017	3.7277	-0.311	0.8172	3.25	173.31	173.34	173.49	173.83	173.49	13.94	23.22	128.1643	0.6003
27....	0.88	0.26	0.018	3.7260	-0.319	0.8170	3.60	173.43	173.46	173.62	173.95	173.61	13.67	22.85	128.2058	0.5982
28....	0.88	0.26	0.018	3.7268	-0.308	0.8239	4.10	171.23	171.28	171.43	171.76	171.42	13.16	22.14	128.1956	0.5944
29....	0.88	0.26	0.018	3.7276	-0.297	0.8312	4.60	168.98	169.03	169.18	169.52	169.17	12.64	21.42	128.1981	0.5901
30....	0.88	0.26	0.019	3.7247	-0.320	0.8206	4.25	172.32	172.36	172.51	172.84	172.50	13.11	22.07	128.2290	0.5940
31....	0.88	0.26	0.019	3.7256	-0.309	0.8276	4.75	170.14	170.20	170.34	170.68	170.34	12.61	21.38	128.2470	0.5898
32....	0.88	0.26	0.019	3.7264	-0.298	0.8349	5.25	167.90	167.97	168.11	168.44	168.10	12.10	20.66	128.2388	0.5857
33....	0.88	0.26	0.019	3.7272	-0.287	0.8427	5.75	165.61	165.69	165.83	166.16	165.82	11.58	19.94	128.2763	0.5807
34....	0.88	0.26	0.019	3.7277	-0.281	0.8467	6.00	164.45	164.53	164.67	165.00	164.66	11.31	19.57	128.2869	0.5779
35....	0.88	0.27	0.020	3.7267	-0.319	0.8135	3.50	174.60	174.63	174.78	175.11	174.78	13.72	22.93	128.2413	0.5983
36....	0.88	0.27	0.020	3.7272	-0.314	0.8170	3.75	173.49	173.52	173.67	174.00	173.67	13.47	22.57	128.2501	0.5968
37....	0.88	0.27	0.020	3.7277	-0.307	0.8212	4.05	172.13	172.17	172.32	172.65	172.31	13.16	22.14	128.2283	0.5944
38....	0.88	0.27	0.021	3.7257	-0.319	0.8179	4.20	173.23	173.27	173.42	173.75	173.41	13.11	22.07	128.2698	0.5940
39....	0.88	0.27	0.021	3.7259	-0.316	0.8200	4.35	172.57	172.61	172.76	173.09	172.75	12.95	21.86	128.2741	0.5924
40....	0.88	0.27	0.021	3.7265	-0.308	0.8250	4.70	171.00	171.05	171.19	171.52	171.19	12.59	21.36	128.2801	0.5894
41....	0.88	0.27	0.021	3.7273	-0.297	0.8325	5.20	168.70	168.76	168.90	169.22	168.89	12.07	20.63	128.2863	0.5851
42....	0.88	0.27	0.021	3.7277	-0.292	0.8356	5.40	167.76	167.83	167.97	168.29	167.96	11.86	20.34	128.2932	0.5831
43....	0.89	0.26	0.018	3.7272	-0.319	0.8122	2.40	175.96	175.97	176.13	176.46	176.13	14.68	24.23	128.9222	0.6059
44....	0.89	0.26	0.018	3.7277	-0.313	0.8155	2.65	174.87	174.88	175.04	175.37	175.04	14.43	23.88	128.9060	0.6043
45....	0.89	0.26	0.019	3.7260	-0.319	0.8162	3.05	174.71	174.73	174.89	175.22	174.88	14.09	23.41	128.9541	0.6019
46....	0.89	0.26	0.019	3.7265	-0.313	0.8202	3.35	173.42	173.45	173.60	173.93	173.60	13.79	23.00	128.9524	0.5996
47....	0.89	0.26	0.019	3.7270	-0.306	0.8244	3.65	172.10	172.13	172.28	172.61	172.28	13.49	22.57	128.9561	0.5977
48....	0.89	0.26	0.019	3.7276	-0.299	0.8294	4.00	170.54	170.58	170.73	171.06	170.72	13.13	22.07	128.9527	0.5949
49....	0.89	0.26	0.020	3.7249	-0.319	0.8205	3.75	173.36	173.39	173.54	173.87	173.54	13.48	22.56	128.9785	0.5975
50....	0.89	0.26	0.020	3.7254	-0.313	0.8246	4.05	172.07	172.11	172.26	172.59	172.25	13.18	22.15	128.9805	0.5950
51....	0.89	0.26	0.020	3.7257	-0.308	0.8274	4.25	171.20	171.24	171.39	171.72	171.38	12.98	21.86	128.9833	0.5938
52....	0.89	0.26	0.020	3.7266	-0.298	0.8347	4.75	168.98	169.03	169.17	169.50	169.17	12.47	21.16	129.0087	0.5893
53....	0.89	0.26	0.020	3.7274	-0.286	0.8422	5.25	166.71	166.78	166.91	167.24	166.91	11.95	20.44	129.0046	0.5846
54....	0.89	0.26	0.020	3.7276	-0.283	0.8446	5.40	166.02	166.09	166.22	166.55	166.22	11.19	20.22	129.0209	0.5534

Table 3
-Continued

Model	M			log L		R		Age							r_{01}	
	(M_\odot)	Y_i	Z_i	$\log T_{eff}$	(L_\odot)	(R_\odot)	(Gyr)	$\langle \Delta\nu_0 \rangle$	$\langle \Delta\nu_1 \rangle$	$\langle \Delta\nu_2 \rangle$	$\langle \Delta\nu_3 \rangle$	$\langle \Delta\nu \rangle$	$\langle \delta\nu_{02} \rangle$	$\langle \delta\nu_{13} \rangle$	$\langle \Delta\nu_r \rangle$	
55.....	0.89	0.26	0.021	3.7238	-0.319	0.8247	4.45	172.08	172.13	172.27	172.60	172.27	12.88	21.73	129.0190	0.5927
56.....	0.89	0.26	0.021	3.7246	-0.309	0.8316	4.95	169.94	169.99	170.13	170.46	170.13	12.38	21.04	129.0187	0.5884
57.....	0.89	0.26	0.021	3.7255	-0.298	0.8389	5.45	167.73	167.80	167.94	168.26	167.93	11.88	20.34	129.0309	0.5841
58.....	0.89	0.26	0.021	3.7263	-0.286	0.8466	5.95	165.47	165.55	165.67	166.00	165.67	11.36	19.63	129.0510	0.5787
59.....	0.89	0.26	0.021	3.7271	-0.275	0.8547	6.45	163.14	163.24	163.36	163.69	163.35	10.84	18.90	129.0743	0.5735
60.....	0.89	0.26	0.021	3.7277	-0.267	0.8606	6.80	161.48	161.59	161.70	162.04	161.70	10.48	18.39	129.0958	0.5699
61.....	0.89	0.27	0.021	3.7269	-0.319	0.8132	3.00	175.72	175.74	175.89	176.22	175.89	14.11	23.44	128.9844	0.6020
62.....	0.89	0.27	0.021	3.7276	-0.309	0.8195	3.45	173.71	173.74	173.89	174.21	173.88	13.65	22.80	128.9951	0.5987
63.....	0.90	0.26	0.019	3.7273	-0.319	0.8118	1.90	177.12	177.13	177.29	177.62	177.29	15.07	24.75	129.6755	0.6089
64.....	0.90	0.26	0.019	3.7276	-0.315	0.8144	2.10	176.24	176.26	176.42	176.74	176.41	14.87	24.47	129.6522	0.6077
65.....	0.90	0.26	0.020	3.7261	-0.319	0.8159	2.55	175.82	175.84	175.99	176.32	175.99	14.47	23.92	129.7010	0.6049
66.....	0.90	0.26	0.020	3.7270	-0.308	0.8233	3.10	173.44	173.47	173.62	173.94	173.61	13.92	23.15	129.6916	0.6013
67.....	0.90	0.26	0.020	3.7276	-0.300	0.8282	3.45	171.90	171.93	172.08	172.40	172.07	13.56	22.66	129.6904	0.5984
68.....	0.90	0.26	0.021	3.7250	-0.319	0.8203	3.25	174.43	174.46	174.61	174.93	174.60	13.85	23.05	129.7189	0.6009
69.....	0.90	0.26	0.021	3.7254	-0.314	0.8237	3.50	173.37	173.39	173.54	173.87	173.54	13.60	22.71	129.7338	0.5989
70.....	0.90	0.26	0.021	3.7259	-0.308	0.8271	3.75	172.29	172.32	172.46	172.79	172.46	13.35	22.36	129.7255	0.5970
71.....	0.90	0.26	0.021	3.7267	-0.298	0.8342	4.25	170.09	170.13	170.27	170.60	170.27	12.84	21.66	129.7309	0.5928
72.....	0.90	0.26	0.021	3.7276	-0.285	0.8424	4.80	167.62	167.67	167.81	168.13	167.80	12.28	20.87	129.7387	0.5884
73.....	0.91	0.26	0.020	3.7274	-0.319	0.8112	1.40	178.34	178.35	178.51	178.84	178.51	15.46	25.28	130.4231	0.6116
74.....	0.91	0.26	0.020	3.7277	-0.315	0.8138	1.60	177.46	177.47	177.63	177.95	177.62	15.26	25.00	130.3972	0.6104
75.....	0.91	0.26	0.021	3.7262	-0.319	0.8154	2.05	176.98	176.99	177.15	177.47	177.14	14.85	24.43	130.4286	0.6079
76.....	0.91	0.26	0.021	3.7270	-0.309	0.8221	2.55	174.82	174.84	174.99	175.31	174.99	14.36	23.74	130.4368	0.6049
77.....	0.91	0.26	0.021	3.7277	-0.300	0.8277	2.95	173.07	173.09	173.24	173.56	173.24	13.95	23.17	130.4541	0.6021
78.....	0.85	0.29	0.022	3.7244	-0.353	0.7914	4.05	178.88	178.91	179.06	179.39	179.06	13.56	22.78	126.0645	0.5953
79.....	0.85	0.29	0.022	3.7261	-0.332	0.8045	5.00	174.56	174.62	174.75	175.08	174.75	12.59	21.42	126.0974	0.5878
80.....	0.85	0.29	0.022	3.7277	-0.310	0.8195	6.00	169.78	169.87	169.99	170.32	169.99	11.52	19.94	126.1092	0.5777
81.....	0.86	0.28	0.022	3.7248	-0.323	0.8176	5.70	171.40	171.47	171.60	171.93	171.60	11.91	20.46	126.8611	0.5821
82.....	0.86	0.28	0.022	3.7262	-0.305	0.8297	6.50	167.68	167.77	167.89	168.22	167.89	11.08	19.31	126.8839	0.5738
83.....	0.86	0.28	0.022	3.7277	-0.284	0.8446	7.40	163.28	163.40	163.51	163.85	163.51	10.13	17.97	126.9173	0.5637
84.....	0.87	0.28	0.022	3.7263	-0.321	0.8141	4.55	173.48	173.53	173.67	174.00	173.67	12.82	21.70	127.5679	0.5908
85.....	0.87	0.28	0.022	3.7270	-0.312	0.8199	4.95	171.66	171.72	171.85	172.18	171.85	12.41	21.13	127.5824	0.5873
86.....	0.87	0.28	0.022	3.7277	-0.303	0.8260	5.35	169.78	169.84	169.98	170.30	169.97	11.99	20.54	127.5975	0.5837
87.....	0.88	0.27	0.022	3.7244	-0.322	0.8208	4.80	172.37	172.43	172.57	172.89	172.56	12.61	21.38	128.3205	0.5898
88.....	0.88	0.27	0.022	3.7261	-0.299	0.8354	5.80	167.89	167.97	168.09	168.42	168.09	11.59	19.96	128.3464	0.5807
89.....	0.88	0.27	0.022	3.7278	-0.276	0.8516	6.80	162.92	163.02	163.13	163.47	163.13	10.49	18.42	128.1998	0.5695
90.....	0.89	0.26	0.022	3.7244	-0.297	0.8439	6.20	166.32	166.41	166.53	166.86	166.53	11.26	19.48	129.1008	0.5780
91.....	0.89	0.26	0.022	3.7251	-0.288	0.8500	6.60	164.54	164.64	164.76	165.08	164.75	10.86	18.92	129.1082	0.5740
92.....	0.89	0.26	0.022	3.7258	-0.279	0.8564	7.00	162.70	162.81	162.92	163.25	162.92	10.45	18.35	129.1188	0.5695
93.....	0.89	0.27	0.022	3.7257	-0.320	0.8171	3.65	174.52	174.55	174.70	175.02	174.69	13.53	22.63	129.0271	0.5979
94.....	0.89	0.27	0.022	3.7267	-0.308	0.8248	4.20	172.10	172.14	172.28	172.60	172.28	12.97	21.86	129.0500	0.5933
95.....	0.89	0.27	0.022	3.7277	-0.295	0.8336	4.80	169.36	169.42	169.55	169.87	169.55	12.35	20.99	129.0430	0.5884
96.....	0.90	0.26	0.022	3.7245	-0.312	0.8294	4.30	171.64	171.68	171.82	172.14	171.82	12.90	21.73	129.7836	0.5936
97.....	0.90	0.26	0.022	3.7262	-0.291	0.8431	5.25	167.49	167.55	167.68	168.00	167.68	11.94	20.41	129.8075	0.5850
98.....	0.90	0.26	0.022	3.7277	-0.269	0.8581	6.20	163.12	163.21	163.33	163.65	163.33	10.96	19.04	129.8293	0.5756
99.....	0.90	0.27	0.022	3.7274	-0.314	0.8164	2.75	175.74	175.76	175.91	176.23	175.91	14.23	23.59	129.7612	0.6032
100....	0.90	0.27	0.022	3.7276	-0.312	0.8177	2.85	175.32	175.34	175.49	175.81	175.49	14.14	23.45	129.7608	0.6030
101....	0.90	0.27	0.022	3.7277	-0.311	0.8183	2.90	175.10	175.12	175.27	175.59	175.27	14.09	23.39	129.7408	0.6023
102....	0.91	0.26	0.022	3.7251	-0.320	0.8194	2.70	175.76	175.78	175.93	176.25	175.93	14.27	23.62	130.4920	0.6041
103....	0.91	0.26	0.022	3.7264	-0.304	0.8302	3.50	172.34	172.36	172.51	172.83	172.51	13.48	22.51	130.4933	0.5988
104....	0.91	0.26	0.022	3.7277	-0.286	0.8418	4.30	168.79	168.83	168.97	169.29	168.97	12.66	21.38	130.5037	0.5921
105....	0.92	0.26	0.022	3.7271	-0.309	0.8222	2.10	175.80	175.81	175.97	176.28	175.97	14.69	24.18	131.1912	0.6075
106....	0.92	0.26	0.022	3.7274	-0.306	0.8243	2.25	175.16	175.17	175.32	175.64	175.32	14.54	23.97	131.2077	0.6066
107....	0.92	0.26	0.022	3.7277	-0.303	0.8263	2.40	174.51	174.52	174.67	174.99	174.67	14.39	23.76	131.1973	0.6056
108....	0.85	0.29	0.023	3.7258	-0.320	0.8169	6.25	170.64	170.72	170.84	171.17	170.84	11.41	19.79	126.1371	0.5766
109....	0.85	0.29	0.023	3.7265	-0.312	0.8223	6.60	168.97	169.06	169.17	169.51	169.18	11.04	19.28	126.1521	0.5726
110....	0.85	0.29	0.023	3.7271	-0.302	0.8288	7.00	167.00	167.11	167.21	167.55	167.22	10.61	18.68	126.1720	0.5680
111....	0.86	0.28	0.023	3.7244	-0.314	0.8276	6.80	168.35	168.44	168.55	168.89	168.56	10.93	19.10	126.9069	0.5723
112....	0.86	0.28	0.023	3.724												

Table 3
-Continued

Model	M			$\log T_{eff}$	(L_\odot)	R	Age			$\langle \Delta\nu_0 \rangle$	$\langle \Delta\nu_1 \rangle$	$\langle \Delta\nu_2 \rangle$	$\langle \Delta\nu_3 \rangle$	$\langle \Delta\nu \rangle$	$\langle \delta\nu_{02} \rangle$	$\langle \delta\nu_{13} \rangle$	$\langle \Delta\nu_r \rangle$	r_{01}
	(M_\odot)	Y_i	Z_i				$\langle \Delta\nu_0 \rangle$	$\langle \Delta\nu_1 \rangle$	$\langle \Delta\nu_2 \rangle$									
113....	0.86	0.28	0.023	3.7248	-0.310	0.8307	7.00	167.42	167.52	167.63	167.96	167.63	10.72	18.82	126.9165	0.5696		
114....	0.87	0.28	0.023	3.7258	-0.314	0.8228	5.55	170.78	170.85	170.98	171.30	170.98	11.91	20.44	127.6106	0.5827		
115....	0.87	0.28	0.023	3.7268	-0.300	0.8319	6.15	168.00	168.08	168.20	168.52	168.20	11.29	19.57	127.6241	0.5769		
116....	0.87	0.28	0.023	3.7278	-0.286	0.8417	6.75	165.10	165.20	165.31	165.64	165.31	10.65	18.68	127.6542	0.5701		
117....	0.88	0.27	0.023	3.7246	-0.305	0.8358	6.25	167.81	167.89	168.01	168.34	168.01	11.27	19.52	128.3774	0.5774		
118....	0.88	0.27	0.023	3.7252	-0.297	0.8411	6.60	166.24	166.33	166.44	166.77	166.45	10.91	19.03	128.3971	0.5733		
119....	0.88	0.27	0.023	3.7258	-0.288	0.8475	7.00	164.37	164.47	164.58	164.91	164.59	10.50	18.46	128.4142	0.5688		
120....	0.89	0.27	0.023	3.7257	-0.307	0.8299	4.95	170.55	170.60	170.74	171.06	170.74	12.32	20.96	129.0845	0.5878		
121....	0.89	0.27	0.023	3.7267	-0.293	0.8388	5.55	167.83	167.90	168.03	168.35	168.03	11.70	20.10	129.0846	0.5821		
122....	0.89	0.27	0.023	3.7277	-0.280	0.8484	6.15	165.02	165.11	165.22	165.54	165.22	11.07	19.22	129.1111	0.5760		
123....	0.90	0.26	0.023	3.7246	-0.297	0.8436	5.70	167.37	167.44	167.57	167.89	167.57	11.62	19.96	129.8378	0.5821		
124....	0.90	0.26	0.023	3.7257	-0.282	0.8535	6.35	164.49	164.57	164.69	165.01	164.69	10.96	19.05	129.8591	0.5753		
125....	0.90	0.26	0.023	3.7267	-0.269	0.8633	6.95	161.71	161.81	161.92	162.25	161.92	10.34	18.18	129.8802	0.5688		
126....	0.90	0.26	0.023	3.7268	-0.267	0.8641	7.00	161.47	161.57	161.68	162.01	161.68	10.29	18.11	129.8680	0.5682		
127....	0.91	0.26	0.023	3.7257	-0.298	0.8381	4.45	169.93	169.97	170.11	170.42	170.11	12.62	21.33	130.5190	0.5917		
128....	0.91	0.26	0.023	3.7267	-0.285	0.8470	5.05	167.28	167.34	167.47	167.78	167.47	12.01	20.49	130.5456	0.5861		
129....	0.91	0.26	0.023	3.7277	-0.271	0.8564	5.65	164.54	164.61	164.73	165.05	164.73	11.39	19.62	130.5533	0.5805		

Note.—The above mean large separations were calculated averaging over n=10, 11, 22, ..., 30. The mean small separations were averages over n=10, 11, 12, ..., 30 at a fixed l (as indicated).